ORGANIC LETTERS

2012
Vol. 14, No. 21
5396–5399

Structure of FD-895 Revealed through Total Synthesis

Reymundo Villa, Alexander L. Mandel, Brian D. Jones, James J. La Clair, and Michael D. Burkart*

Department of Chemistry and Biochemistry, University of Calfornia, San Diego, 9500 Gilman Drive, La Jolla, California 92093-0358, United States

mburkart@ucsd.edu

Received August 17, 2012

ABSTRACT

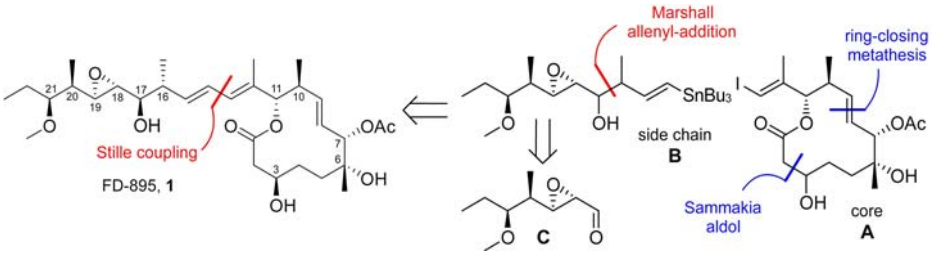

The total synthesis of FD-895 was completed through a strategy that featured the use of a tandem esterification ring-closing metathesis (RCM) process to construct the 12-membered macrolide and a modified Stille coupling to append the side chain. These studies combined with detailed analysis of all four possible C16−C17 stereoisomers were used to confirm the structure of FD-895 and identify an analog with an enhanced subnanomolar bioactivity.

First described in 1994, FD-895 (**1**, Figure 1) introduced a family of 12-membered macrolides identified with potent cytostatic activity during hypoxia response.[1] A decade later, studies at Eisai Co. Ltd. led to the isolation of related macrolides including pladienolides B (**2a**) and D (**2b**).[2] In 2007, the complete structure of **2b** (Figure 1) was reported[3] and confirmed by total synthesis.[4] Fueled by a series of mode of action studies,[5] the entry into clinical trials of E7107 (**2c**)[6] sparked wide interest in the spliceosome as a new chemotherapeutic target (Figure 1).[7] The early suspension of this trial suggests the need for further studies into this potent class of macrolides. The planar structure and in vitro cytotoxicity of FD-895 (**1**) was reported in 1994.[1] We now report the use of total synthesis to identify and validate the structure of FD-895 (**1**) and apply our synthetic methods to identify analogs with enhanced activity in select tumor cell lines.

Our studies began with evaluating the structure of FD-895 (**1**) by NMR methods to naturally isolated material. After screening solvents, we collected a 2D data set on **1** in C_6D_6, as it provided optimal stability and peak resolution. We first assigned the protons and carbons in **1** using a combination of gCOSY, TOCSY, HSQC, and HMBC data. We then applied proton coupling constants and NOE correlations to evaluate the stereochemistry. Coupling constant analyses confirmed the *cis*- or *trans*- relationships at C8−C9, C10−C11, C14−C15, C18−C19, C20−C21, and C21−C22. Through-ring NOEs obtained from NOESY spectra indicated that the stereochemistry

(1) Seki-Asano, M.; Okazaki, T.; Yamagishi, M.; Sakai, N.; Takayama, Y.; Hanada, K.; Morimoto, S.; Takatsuki, A.; Mizoue, K. J. *Antibiot. (Tokyo)* **1994**, *47*, 1395–1401.

(2) Mizui, Y.; Sakai, T.; Iwata, M.; Uenaka, T.; Okamoto, K.; Shimizu, H.; Yamori, T.; Yoshimatsu, K.; Asada, M. *J. Antibiot. (Tokyo)* **2004**, *57*, 188–196.

(3) Asai, N.; Kotake, Y.; Niijima, J.; Fukuda, Y.; Uehara, T.; Sakai, T. *J. Antibiot. (Tokyo)* **2007**, *57*, 188–196.

(4) (a) Kanada, R. M.; Itoh, D.; Nagai, M.; Niijima, J.; Asai, N.; Mizui, Y.; Abe, S.; Kotake, Y. *Angew. Chem., Int. Ed.* **2007**, *46*, 4350–4355. (b) Kanada, R. M.; Itoh, D.; Nagai, M.; Niijima, J.; Asai, N.; Mizui, Y.; Abe, S.; Kotake, Y. *Angew. Chem., Int. Ed.* **2007**, *46*, 8734.

(5) (a) Kotake, Y.; Sagane, K.; Owa, T.; Mimori-Kiyosue, Y.; Shimizu, H.; Uesugi, M.; Ishihama, Y.; Iwata, M.; Mizui, Y. *Nat. Chem. Biol.* **2007**, *3*, 570–575. (b) Kaida, D.; Motoyoshi, H.; Tashiro, E.; Nojima, T.; Hagiwara, M.; Ishigami, K.; Watanabe, H.; Kitahara, T.; Yoshida, T.; Nakajima, H.; Tani, T.; Horinouchi, S.; Yoshida, M. *Nat. Chem. Biol.* **2007**, *3*, 576–583. (c) Yokoi, A.; Kotake, Y.; Takahashi, K.; Kadowaki, T.; Matsumoto, Y.; Minoshima, Y.; Sugi, N. H.; Sagane, K.; Hamaguchi, M.; Iwata, M.; Mizui, Y. *FEBS J.* **2011**, *278*, 4870–4880.

(6) Folco, E. G.; Coil, K. E.; Reed, R. *Genes Dev.* **2011**, *25*, 440–444.

(7) (a) Ward, A. J.; Cooper, T. A. *J. Pathol.* **2010**, *220*, 152–163. (b) Fan, L.; Lagisetti, C.; Edwards, C. C.; Webb, T. R.; Potter, P. M. *ACS Chem. Biol.* **2011**, *6*, 582–589.

10.1021/ol3023006
Published on Web 10/16/2012

at C6, C7, C10, and C11 was comparable to that in pladienolide B (**2a**).[3] While the C16−C17 diad was assigned as *trans*− due to a 12.6 Hz coupling constant for H16−H17, C17−C18 could not be assigned due to the mid-ranged 5.5 Hz coupling constant for H17−H18. After further inspection through examination of 1D and 2D NMR spectra in different solvents, we concluded that centers C3, C16 and C17 could not be unambiguously assigned by NMR methods.

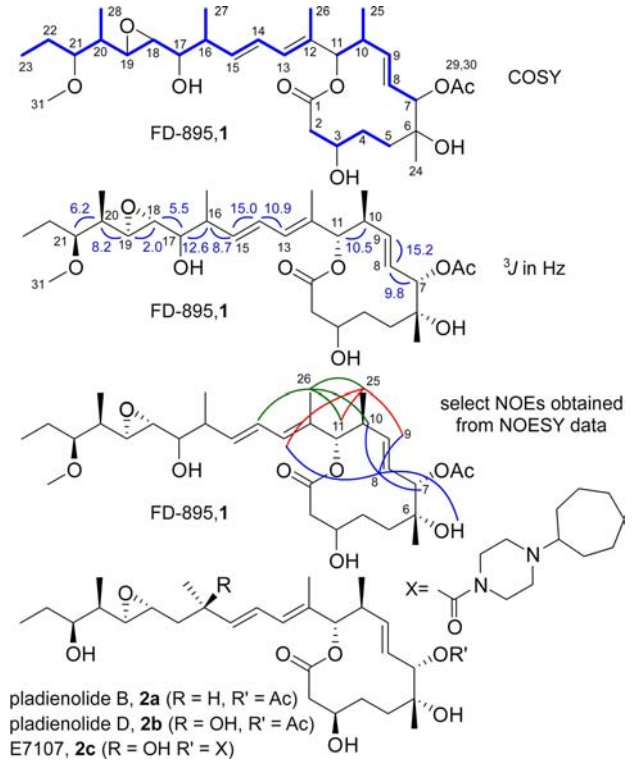

Figure 1. NMR analysis of FD-895 (**1**), in C_6D_6 revealed key COSY interactions, ^3J-coupling constants, and select NOE interactions. FD-895 (**1**) was the first member of a family of 12-memebered ring polyketides that includes pladienolides B (**2a**) and D (**2b**), as well as clinical entry E7107 (**2c**).

While considerable effort was made to determine the structure of **1** via X-ray crystallography and degradative methods, all attempts proved unsuccessful. Based on prior studies on **2a**−**2b**,[3,4] we tentatively assigned C3 as *R*. The quest then remained to validate the stereochemistry within the core (C3, C6, C7, C10, and C11), confirm the assignment in the side chain terminus (at C18−C21), and identify the C16−C17 stereodiad.

We tailored our retrosynthesis such that installation of the unassigned C16−C17 stereocenters occurred at the end of the synthesis (see Abstract).[4b,8] A Stille coupling dissected the molecule into a core vinyl iodide **A** and side chain vinyl stannane **B**.[9] Component **B** was derived by applying a Marshall allenyl−addition[10] to **C** followed by subsequent hydrostannylation, as this method could be tuned to deliver each of the four C16−C17 stereoisomers.

Scheme 1. Construction of Side Chain **8** in 13 Steps and 19% Overall Yield from L-Phe

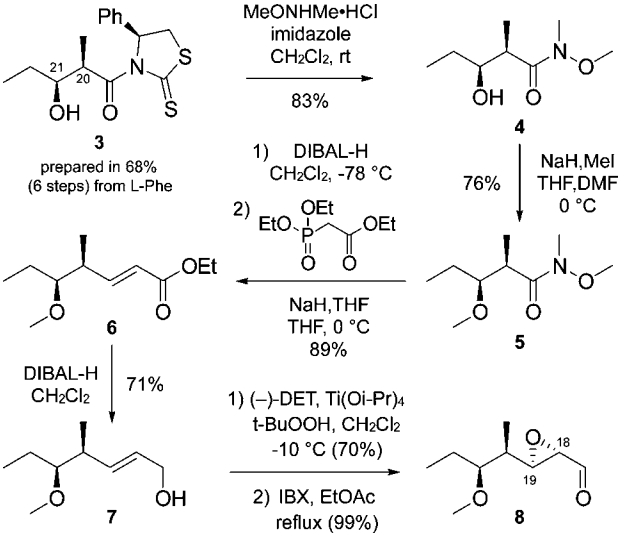

We began with epoxy-aldehyde component **C** by developing a route to prepare aldehyde **8**[8] in 13 steps from L-Phe (Scheme 1). Application of a Crimmins auxiliary set the C20−C21 stereodiad by providing non-Evans *syn*-adduct **3** with ∼5:1 *de*, which after chromatographic purification provided pure **3** in 68% yield.[11]

Conversion of **3** to Weinreb's amide **4** followed by methylation provided amide **5**. Reduction of **5** with DIBAL-H, followed by a Horner−Wadsworth−Emmons olefination,[12] provided ester **6**. Potential isomerization of the α-methyl group in the intermediate aldehyde was avoided by conducting the HWE reaction immediately after isolation of the aldehyde.

Reduction to **7** with DIBAL-H set the stage for installation of the C18−C19 epoxide by a Sharpless epoxidation,[13] which after IBX oxidation[14] completed the synthesis of component **8**. Encouragingly, the coupling constants in **8** were comparable to that at C18−C21 in **1** (see Supporting Information).

Our attention next turned to the core component **A**. Building on our initial route[4b,8] and approaches developed by Kotake, Maier, and Skaanderup,[4,15] we identified a

(8) Synthesis of intermediate **8** and a first-generation demonstration of this approach can be found in: Mandel, A. L.; Jones, B. D.; La Clair, J. J.; Burkart, M. D. *Bioorg. Med. Chem. Lett.* **2007**, *17*, 5159–5164.

(9) Stille, J. K.; Groh, B. L. *J. Am. Chem. Soc.* **1987**, *109*, 813–817.

(10) (a) Marshall, J. A. *J. Org. Chem.* **2007**, *72*, 8153–8166. (b) Marshall, J. A.; Perkins, J. *J. Org. Chem.* **1994**, *59*, 3509–3511.

(11) Crimmins, M. T.; King, B. W.; Tabet, E. A. *J. Am. Chem. Soc.* **1997**, *119*, 7883–7884.

(12) Wadsworth, W. S.; Emmons, W. D. *J. Am. Chem. Soc.* **1961**, *83*, 1733–1738.

(13) Katsuki, T.; Sharpless, K. B. *J. Am. Chem. Soc.* **1980**, *102*, 5974–5976.

(14) More, J. D.; Finney, N. S. *Org. Lett.* **2002**, *4*, 3001–3003.

(15) (a) Müller, S.; Mayer, T.; Sasse, F.; Maier, M. E. *Org. Lett.* **2011**, *13*, 3940–3943. (b) Skaanderup, P. R.; Jensen, T. *Org. Lett.* **2008**, *10*, 2821–2124.

stereoselective route to macrolide **21** that began with Brown addition[16] of the MEM ether **10** to aldehyde **9** in order to set the C7 stereocenter in **11** (Scheme 2).

Scheme 2. Synthesis of Core **21** in 14 Steps and 2% Yield

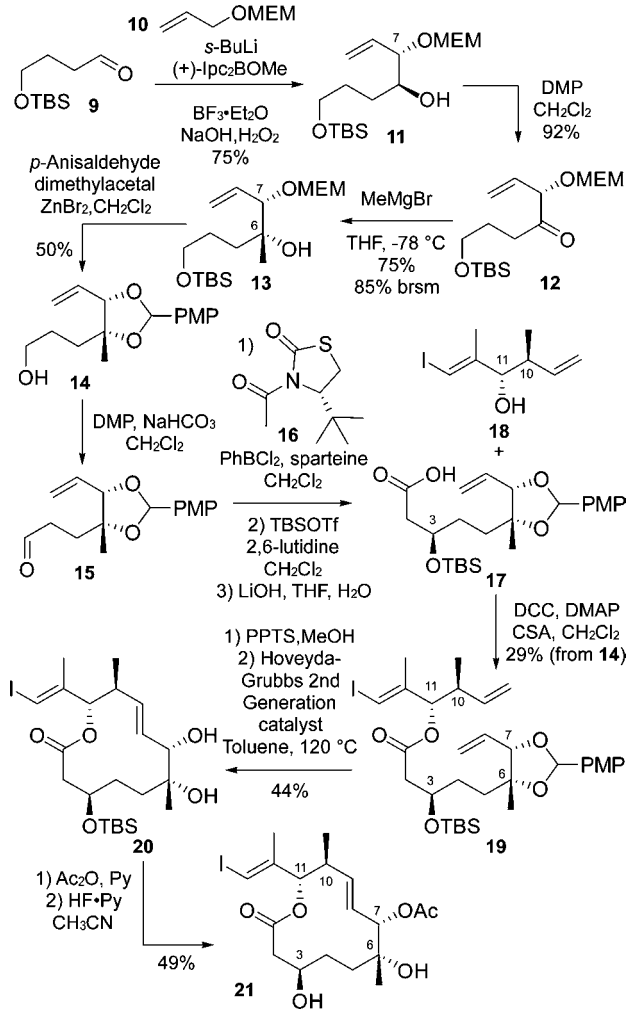

We then used this C7 center to guide the construction at C6 by oxidation of **11** to ketone **12**, followed by a chelate–controlled addition[17] of MeMgBr, to afford adduct **13**. Treatment of **13** with *p*-anisaldehyde dimethylacetal and $ZnBr_2$ both converted the MEM ether to PMP acetal and deprotected the TBS ether in one operation, affording carbinol **14**.

At this stage, we were set to install the C3 center (Scheme 2). Oxidation of **14** to aldehyde **15**, followed by an acetate aldol addition of the Sammakia auxiliary **16**,[18] provided acid **17** after TBS protection and hydrolytic workup. We next applied an esterification and RCM protocol derived from our prior synthetic endeavors.[19,8] Acid **17** was coupled to alcohol **18** to afford ester **19**. The conversion from **14** to **19** was ideally conducted in a single direct sequence without long-term storage or purification. Removal of the PMP acetal enabled the preparation of lactone **20** by means of an RCM reaction using Hoveyda–Grubbs second generation catalyst.[20] The desired core unit **21** was obtained by acylation of the secondary carbinol at C7 and TBS deprotection at C3.

The final objective in our synthesis involved the assembly of components **8** and **21** to prepare the desired C16–C17 stereoisomer in FD-895 (**1**). As the stereochemistry at C16–C17 was not defined, we explored the versatile allenylstannane methods developed by Marshall to prepare each of the possible terminal alkynes **24a**, **24b**, **24c**, and **24d** (Scheme 3).[10] Allenylstannanes **23a** and **23b** were prepared from the respective mesylates **22R** (Scheme 3) and **22S** (not shown). Addition of **23a** or **23b** to **8** in the presence of $BF_3{\bullet}Et_2O$ led to the formation of **24b** or **24d**, respectively, as a single diasteromeric product (Scheme 3). NMR analyses clearly demonstrated that these materials contained a *cis*-configuration at C16–C17, as given by a $^3J_{HH}$ value of 4–5 Hz.

Alkynes **24b** and **24d** were then hydrostannylated[21] to their corresponding vinylstannanes sequentially coupled to core **21** under modified Stille conditions[8] to afford the *cis*-isomers **1RS** and **1SR** from **24b** and **24d**, respectively (Scheme 3). NMR studies indicated that neither matched **1** (Figure 1). ^{1}H NMR, gCOSY, ^{13}C NMR data confirmed that while **1RS** and **1SR** were isomers of **1**, protons H16 and H17 were most likely *trans*, as exemplified by a $^3J_{HH}$ value of 12.6 Hz in **1** versus 4–5 Hz in **1RS** and **1SR**.

We then shifted our focus to the two *trans*-isomers **1SS** and **1RR**. Using a mixture of InI and $Pd(OAc)_2$,[10b] we were able to obtain alkyne **24a** as a single product (>99% de) and in sufficient yield from **22R**. The structure of **24a** was confirmed by a combination of ^{1}H NMR, ^{13}C NMR, gCOSY, and HRMS spectral data. Hydrostannylation and Stille coupling to **21** afforded *trans*-isomer **1SS**. Again, NMR data collected from **1SS** (Figure 2) did not match **1**.

Unfortunately, application of the InI and $Pd(OAc)_2$ conditions to **22S** failed to provide alkyne **24c**. After screening conditions, we found that treating mixtures of **23b** and **8** with $SnCl_4$ at −78 °C in hexane[10b] provided **24c** in 83% yield (Scheme 3). Hydrostannylation **24c** followed by Stille coupling to **21** afforded the final isomer **1RR**. Fortunately, the spectral properties of this isomer matched those of the natural material (Figure 2), confirming the synthesis of FD-895 (**1**) in 30 total steps, with the longest linear sequence of 15 steps. All but one of the steps, preparation of **3**, occurred with high stereocontrol (>99% *de*).

Finally, cytotoxicity analyses via the MTT assay[22] indicated that all four isomers displayed sub-nM to nM

(16) Ramachandran, P. V.; Liu, H.; Ram Reddy, M. V.; Brown, H. C. *Org. Lett.* **2003**, *5*, 3755–3757.
(17) Still, W. C.; McDonald, J. H. *Tetrahedron Lett.* **1980**, *21*, 1031–1034.
(18) Zhang, Y.; Phillips, A. J.; Sammakia, T. *Org. Lett.* **2003**, *6*, 23–25.
(19) Ko, K. S.; Alexander, M. D.; Fontaine, S. D.; Biggs-Houck, J. E.; La Clair, J. J.; Burkart, M. D. *Org. Biomol. Chem.* **2010**, *8*, 5159–5165.
(20) Stewart, I. C.; Ung, T.; Pletnev, A. A.; Berlin, J. M.; Grubbs, R. H.; Schrodi, Y. *Org. Lett.* **2007**, *9*, 1589–1592.
(21) Ichinose, Y.; Oda, H.; Oshima, K.; Utimoto, K. *Bull. Chem. Soc. Jpn.* **1987**, *60*, 3468–3470.
(22) Mosmann, T. *J. Immunol. Meth.* **1983**, *65*, 55–83.

Scheme 3. Syntheses of the Four C16−C17 Stereoisomers **1SS**, **1RS**, **1RR**, and **1SR**

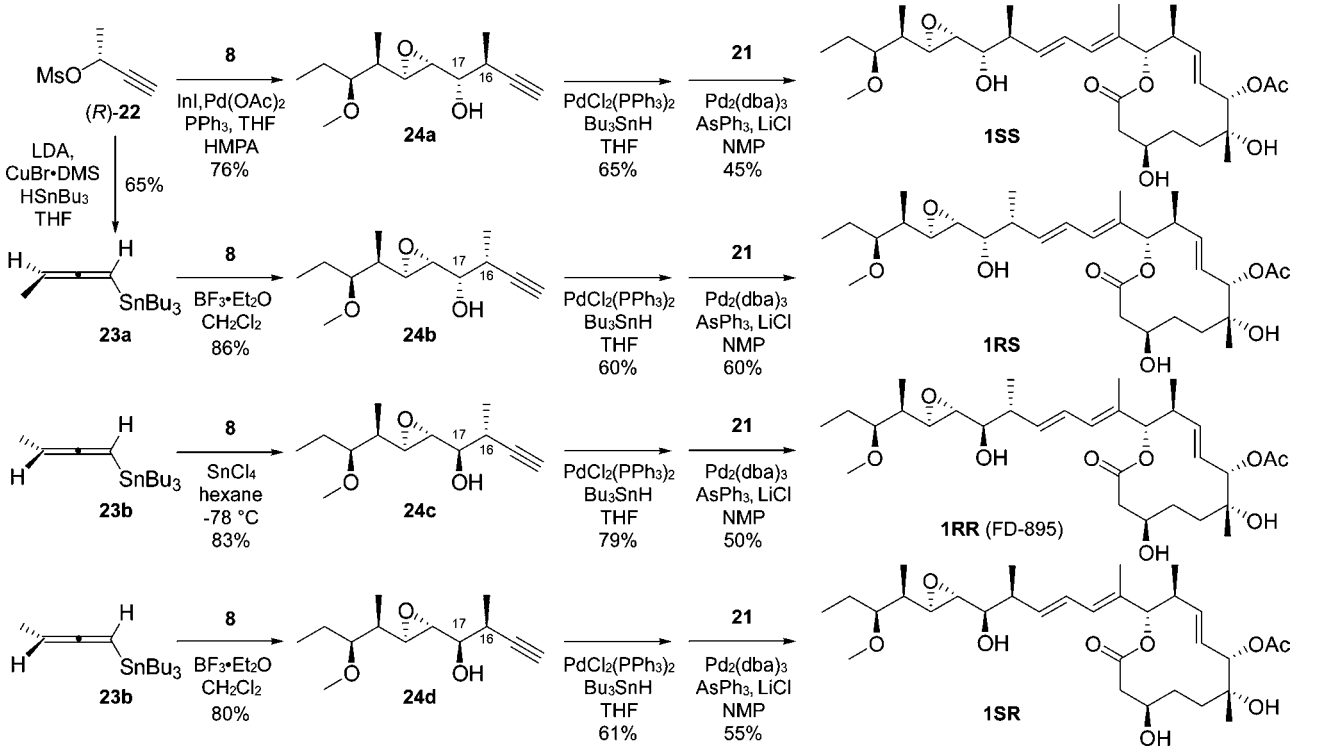

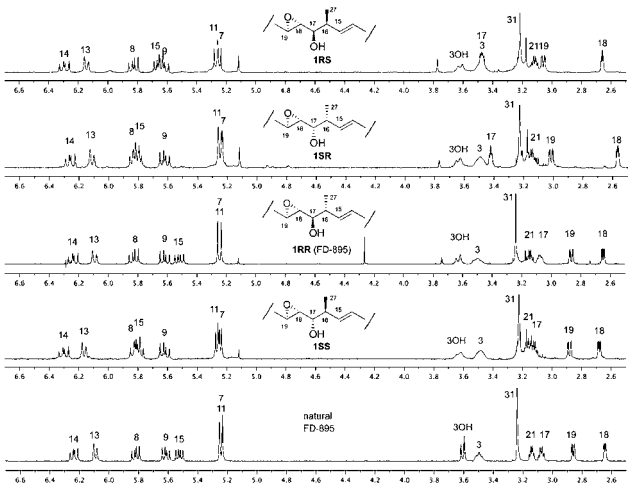

Figure 2. ^{1}H NMR spectra of synthetic isomers **1SS**, **1RS**, **1RR**, **1SR** in C_6D_6 indicated that **1RR** matched natural FD-895 (**1**).

activity when screened against the HCT-116 tumor cell line (IC_{50} value of 23.0 ± 1.2 nM for **1SS**, 0.80 ± 0.05 nM for **1RS**, 24.2 ± 0.9 nM for **1RR**, and 3.7 ± 0.2 nM for **1SR**). While the activity for **1RR** matched that of natural FD-895 (IC_{50} value of 23.5 ± 0.2 nM), isomers with the natural *R*-configuration at C16 were less active than those with *S* at C16. Additional activity was also observed when C17 was left in its natural *R* configuration. Remarkably, isomer **1RS** was nearly 25 times more active than FD-895 (**1**), providing a strong foundation for further medicinal chemical optimization.

Acknowledgment. This work was financially supported by the American Cancer Society (RSG-06-011-01-CDD) and the NIH (3R01GM086225-01S1).

Supporting Information Available. Experimental procedures, characterization data for all new compounds, and full acknowledgments. This material is available free of charge via the Internet at http://pubs.acs.org.

The authors declare no competing financial interest.